JEMT 6 (2018) 38-45 ISSN 2053-3535

Journal of Engineering and Manufacturing Technology
www.bluepenjournals.org/jemt

# Solubility of Pranlukast in isopropanol and isopropanol-*N*,*N*-dimethylformamide binary solvents at different temperatures

**Minghuang Hong†, Kai Wang†, Sai Guo and Guobin Ren***

Laboratory of Pharmaceutical Crystal Engineering and Technology, School of Pharmacy, East China University of Science and Technology, Shanghai, 200237, China.

Article History
Received 13 March, 2018
Received in revised form 12 April, 2018
Accepted 16 April, 2018

**Keywords:**
**Pranlukast, Isopropanol-*N*,*N*-imethylformamide, Thermodynamics properties.**

**Article Type:**
***Full Length Research Article***

**ABSTRACT**

**The solubility of Pranlukast in isopropanol and isopropanol-*N*,*N*-dimethylformamide binary solvents from 293.15 to 333.15 K at atmospheric pressure was determined by dynamic laser method. The results obtained show that the solubility of Pranlukast increased with increasing temperature in a certain solvent system, and also increased with increasing mole fraction of *N*,*N*-dimethylformamide in the binary solvent systems at a specific temperature. Experimental data were correlated using the modified Apelblat model, the CNIBS/Redlich-Kister model and the 3D Jouyban-Acree model. The results obtained suggest that all the models provided good fit, with the most accurate prediction obtained from the modified Apelblat model. Thermodynamic properties including standard enthalpy, standard entropy and molar Gibbs free energy change of solution were calculated as well, which indicated that the dissolution process was endothermic and non-spontaneous.**



## INTRODUCTION

Pranlukast {N-[4-oxo-2-(1H-tetrazol-5-yl)-4H-chromen-7-yl]-4-(4-phenylbutoxy)benzamide, PRS, Figure 1} is a potent selective cysteniyl leukotriene receptor antagonist to treat bronchial asthma and allergic rhinitis (Yoshihara, 2013). PRS exist in four crystalline forms: the hemihydrate form (HH), the anhydrous form I, the anhydrous form II and the anhydrous form III. The most stable form of PRS in the market is hemihydrate form which was investigated in this work (Furuta et al., 2015a, b). Crystallization is an important step for separation and purification of drug substances in the pharmaceutical industry, and crystallization conditions have a great impact on the properties of the final product, such as purity, particle size and polymorphism. Fundamental solubility data provide vital information for thermodynamic study to design crystallization process (Hong et al., 2016; Yu et al., 2007). It should be noted that PRS showed low solubility in commonly used organic solvents such as methanol, ethanol and acetone, while useful solvents for crystallization included isopropanol (*i*-PrOH) and *N*,*N*-dimethylformamide (DMF). There have not been any systematic researches of the solubility of PRS in organic solvents. From various measurement methods of solubility, the dynamic laser method (Ge et al., 2016; Jouyban-Gharamaleki et al., 2014; Qiaoli Chen, 2009; Wang et al., 2013; Zhu et al., 2016) was applied to determine the solubility of PRS in pure *i*-PrOH and the mixture of *i*-PrOH and DMF solvents at atmospheric pressure from 293.15 to 333.15K. Experimental data were correlated by the modified Apelblat equation, the CNIBS/Redlich-Kister model and the 3D Jouyban-Acree model. The standard enthalpy, standard entropy and molar Gibbs free energy change of solution were calculated with the solubility data. The results could help to understand the relationship between the solubility and temperature as well as solvent composition, so as to

*Corresponding author. E-mail: rgb@ecust.edu.cn.
†These authors contributed equally to this work.

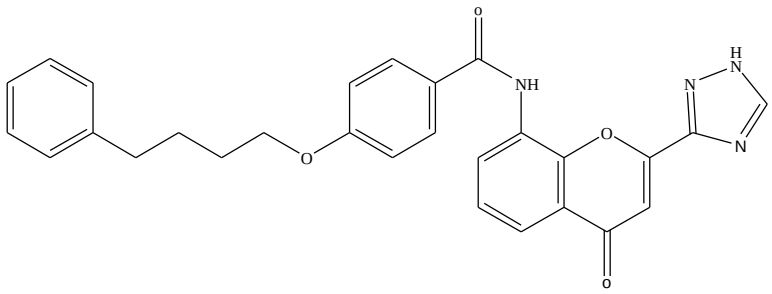

**Figure 1.** Chemical structure of Pranlukast (PRS).

provide guide in separation and purification process of desired PRS crystal form.

## MATERIALS AND METHODS

Pranlukast (PRS) was purchased from Adamas Reagent Co., Ltd. (Shanghai, China), and the purity was more than 99%. DMF and *i*-PrOH, with the purity of greater than 99.5%, were supplied by Shanghai Lingfeng Chemical Reagent Co., Ltd. (Shanghai, China).

The solubility of PRS in pure *i*-PrOH and *i*-PrOH/DMF was measured by dynamic laser method (Li et al., 2012, 2016; Zhi et al., 2016; Qiaoli Chen, 2009; Wang et al., 2013) at atmospheric pressure ranging from 293.15 to 333.15K. The apparatus contained a laser monitor and a 50 mL jacketed glass vessel. In order to provide constant temperature and stirring, it was also equipped with a thermostatic bath and a magnetic stirrer. A mercury thermometer was used to measure the real temperature of the solution. Moreover, an electronic analytical balance with an accuracy of ±0.01 mg was applied to determine the mass of solvent and solute. Allihn condenser was used to prevent the evaporation of solvent.

### Procedure

A small amount of solute powder was added into the solvent, and the mixture was stirred continuously at a constant temperature with the uncertainty of ±0.1 K. As the particles of the solute were dissolving, the signal indicating the number of particles decreased gradually and reached a maximal value when the solute was completely dissolved. Then another mass of the solute was dispensed into the vessel, and the procedure was repeated until the laser monitor could not return to the maximal value, which means the last added powder could not be dissolved. The consumed solute mass was recorded to calculate the mole fraction solubility of PRS ($x_A$) and each experiment was conducted three times.

## RESULTS AND DISCUSSION

### Solubility data

The solubility of PRS in pure *i*-PrOH solvent and *i*-PrOH/DMF mixture solvents were listed in Table 1. These data were also plotted in Figure 2. It was concluded that in a certain solvent system, with the increasing of the temperature, the mole fraction solubility was also increasing. In addition, the mole fraction solubility increased along with the increase of the mole fraction of DMF at a specific temperature.

### Solubility models

Many models have been successfully used in correlating and predicting the solubility in a specific solvent system. Herein, the modified Apelblat equation, CNIBS/R-K model and the 3D Jouyban-Acree model were chosen to correlate the experimental data.

#### *Modified Apelblat equation*

The modified Apelblat equation was proposed by Apelblat and his colleagues to discuss the relationship of solubility and temperature in different solvents. It was expressed as:

$$lnx_A = A + \frac{B}{T} + ClnT \quad (1)$$

Where $x_A$ is the mole fraction solubility of PRS, and *A*, *B* and *C* are semi empirical constants. *A* and *B* represent the change of solution activity coefficients, and *C* represents the effect of temperature on the fusion enthalpy (Li et al., 2012).

#### *Combined nearly ideal binary solvent/Redlich-Kister model*

To study solubility of solute in mixture solvents, Acree

**Table 1.** The mole fraction solubility of PRS ($x_A$) in *i*-PrOH and *i*-PrOH/DMF binary solvents from 293.15K to 333.15 K at atmospheric pressure.

| T/K | $10^4$ | $10^4$ (Equation 1) | $10^4$ (Equation 3) | $10^4$ (Equation 7) |
|---|---|---|---|---|
| $x_B^0$=0 | | | | |
| 293.15 | 0.0589 | 0.0780 | 0.1420 | 0.1510 |
| 298.15 | 0.0966 | 0.1210 | 0.1190 | 0.2020 |
| 303.15 | 0.1849 | 0.1820 | 0.2380 | 0.2680 |
| 308.15 | 0.2242 | 0.2660 | 0.2540 | 0.3510 |
| 313.15 | 0.4334 | 0.3770 | 0.4290 | 0.4570 |
| 318.15 | 0.5626 | 0.5200 | 0.5290 | 0.5900 |
| 323.15 | 0.6886 | 0.6990 | 0.7180 | 0.7550 |
| 328.15 | 0.8627 | 0.9170 | 0.9600 | 0.9600 |
| 333.15 | 1.2001 | 1.1750 | 1.3140 | 1.2110 |
| $x_B^0$=0.05 | | | | |
| 293.15 | 0.2428 | 0.2350 | 0.2270 | 0.2450 |
| 298.15 | 0.2863 | 0.3000 | 0.2630 | 0.3260 |
| 303.15 | 0.3822 | 0.3830 | 0.3820 | 0.4290 |
| 308.15 | 0.5352 | 0.4900 | 0.4630 | 0.5600 |
| 313.15 | 0.5853 | 0.6290 | 0.6720 | 0.7240 |
| 318.15 | 0.7982 | 0.8070 | 0.8480 | 0.9290 |
| 323.15 | 1.0559 | 1.0380 | 1.1360 | 1.1820 |
| 328.15 | 1.3348 | 1.3350 | 1.5330 | 1.4940 |
| 333.15 | 1.7169 | 1.7190 | 1.9890 | 1.8740 |
| $x_B^0$=0.10 | | | | |
| 293.15 | 0.5533 | 0.4890 | 0.3970 | 0.4020 |
| 298.15 | 0.5720 | 0.6070 | 0.5250 | 0.5300 |
| 303.15 | 0.7544 | 0.7600 | 0.6420 | 0.6930 |
| 308.15 | 0.9239 | 0.9590 | 0.8200 | 0.8980 |
| 313.15 | 1.2375 | 1.2200 | 1.0720 | 1.1540 |
| 318.15 | 1.5032 | 1.5630 | 1.3740 | 1.4710 |
| 323.15 | 2.0874 | 2.0150 | 1.8260 | 1.8620 |
| 328.15 | 2.6112 | 2.6140 | 2.4000 | 2.3400 |
| 333.15 | 3.3993 | 3.4100 | 3.0230 | 2.9210 |
| $x_B^0$=0.15 | | | | |
| 293.15 | 0.6192 | 0.6410 | 0.7130 | 0.6550 |
| 298.15 | 0.8462 | 0.8100 | 0.9540 | 0.8590 |
| 303.15 | 1.0387 | 1.0300 | 1.0920 | 1.1160 |
| 308.15 | 1.3125 | 1.3170 | 1.4030 | 1.4370 |
| 313.15 | 1.7056 | 1.6930 | 1.7190 | 1.8360 |
| 318.15 | 2.1027 | 2.1870 | 2.2190 | 2.3270 |
| 323.15 | 2.8199 | 2.8360 | 2.9270 | 2.9280 |
| 328.15 | 3.8127 | 3.6930 | 3.7000 | 3.6600 |
| 333.15 | 4.7729 | 4.8250 | 4.6090 | 4.5430 |
| $x_B^0$=0.20 | | | | |
| 293.15 | 1.2776 | 1.2870 | 1.2540 | 1.0590 |
| 298.15 | 1.6564 | 1.5320 | 1.6030 | 1.3790 |
| 303.15 | 1.8945 | 1.8510 | 1.8290 | 1.7800 |
| 308.15 | 2.1827 | 2.2670 | 2.3120 | 2.2790 |
| 313.15 | 2.6604 | 2.8140 | 2.7410 | 2.8940 |
| 318.15 | 3.4514 | 3.5340 | 3.5300 | 3.6470 |
| 323.15 | 4.5476 | 4.4890 | 4.6130 | 4.5640 |
| 328.15 | 5.9883 | 5.7600 | 5.6380 | 5.6730 |
| 333.15 | 7.3396 | 7.4630 | 7.0260 | 7.0050 |
| $x_B^0$=0.25 | | | | |
| 293.15 | 2.1148 | 1.9760 | 2.0930 | 1.6850 |
| 298.15 | 2.5537 | 2.4270 | 2.5250 | 2.1800 |
| 303.15 | 2.7915 | 2.9780 | 2.9590 | 2.7960 |

**Table 1.** Contd.

| | | | | |
|---|---|---|---|---|
| 308.15 | 3.6089 | 3.6520 | 3.6600 | 3.5580 |
| 313.15 | 4.2100 | 4.4730 | 4.3080 | 4.4930 |
| 318.15 | 5.5679 | 5.4730 | 5.4890 | 5.6310 |
| 323.15 | 6.9648 | 6.6900 | 7.0860 | 7.0090 |
| 328.15 | 8.0775 | 8.1690 | 8.5010 | 8.6670 |
| 333.15 | 9.9338 | 9.9640 | 10.6620 | 10.6480 |
| $x_B^0$=0.30 | | | | |
| 293.15 | 3.1732 | 3.2760 | 3.2600 | 2.6230 |
| 298.15 | 3.7893 | 3.8900 | 3.7830 | 3.3730 |
| 303.15 | 4.6538 | 4.6590 | 4.5830 | 4.3020 |
| 308.15 | 5.8159 | 5.6240 | 5.5790 | 5.4440 |
| 313.15 | 6.7436 | 6.8380 | 6.6270 | 6.8370 |
| 318.15 | 8.3149 | 8.3700 | 8.3050 | 8.5250 |
| 323.15 | 10.7687 | 10.3090 | 10.5630 | 10.5580 |
| 328.15 | 12.3767 | 12.7700 | 12.6750 | 12.9900 |
| 333.15 | 15.9681 | 15.9010 | 16.0170 | 15.8840 |
| $x_B^0$=0.35 | | | | |
| 293.15 | 4.7757 | 4.7460 | 4.7510 | 3.9820 |
| 298.15 | 5.3887 | 5.6360 | 5.4790 | 5.0920 |
| 303.15 | 6.9042 | 6.7600 | 6.7890 | 6.4600 |
| 308.15 | 8.2625 | 8.1860 | 8.2170 | 8.1330 |
| 313.15 | 10.0413 | 9.9990 | 9.9310 | 10.1630 |
| 318.15 | 12.3202 | 12.3130 | 12.2130 | 12.6110 |
| 323.15 | 15.3058 | 15.2770 | 15.2880 | 15.5450 |
| 328.15 | 18.9273 | 19.0870 | 18.6360 | 19.0400 |
| 333.15 | 24.0729 | 24.0000 | 23.6540 | 23.1780 |
| $x_B^0$=0.40 | | | | |
| 293.15 | 6.6697 | 6.7870 | 6.5910 | 5.8810 |
| 298.15 | 7.8858 | 7.9970 | 7.7950 | 7.4840 |
| 303.15 | 9.5641 | 9.5390 | 9.7040 | 9.4480 |
| 308.15 | 11.4975 | 11.5120 | 11.7740 | 11.8370 |
| 313.15 | 14.2640 | 14.0410 | 14.4610 | 14.7240 |
| 318.15 | 17.3032 | 17.2980 | 17.5010 | 18.1900 |
| 323.15 | 21.4358 | 21.5060 | 21.5900 | 22.3260 |
| 328.15 | 27.0873 | 26.9690 | 26.9010 | 27.2310 |
| 333.15 | 33.9934 | 34.0890 | 34.0520 | 33.0160 |
| $x_B^0$=0.45 | | | | |
| 293.15 | 8.9424 | 9.3460 | 9.0090 | 8.4450 |
| 298.15 | 11.0464 | 11.2090 | 11.0830 | 10.6960 |
| 303.15 | 13.6735 | 13.5340 | 13.6160 | 13.4430 |
| 308.15 | 16.7367 | 16.4450 | 16.5660 | 16.7710 |
| 313.15 | 20.5495 | 20.0980 | 20.4510 | 20.7740 |
| 318.15 | 24.6890 | 24.6930 | 24.5770 | 25.5620 |
| 323.15 | 30.1361 | 30.4860 | 30.0480 | 31.2510 |
| 328.15 | 37.6573 | 37.8090 | 37.8770 | 37.9730 |
| 333.15 | 47.2189 | 47.0840 | 47.3260 | 45.8710 |
| $x_B^0$=0.50 | | | | |
| 293.15 | 12.7747 | 13.0630 | 12.7600 | 11.7910 |
| 298.15 | 16.0330 | 15.7580 | 16.0270 | 14.8730 |
| 303.15 | 19.2466 | 19.0670 | 19.2550 | 18.6180 |
| 308.15 | 23.1286 | 23.1370 | 23.1610 | 23.1370 |
| 313.15 | 28.1209 | 28.1470 | 28.1380 | 28.5540 |
| 318.15 | 34.1183 | 34.3210 | 34.1400 | 35.0070 |
| 323.15 | 41.7990 | 41.9340 | 41.8150 | 42.6480 |
| 328.15 | 51.6407 | 51.3310 | 51.5870 | 51.6460 |
| 333.15 | 62.8365 | 62.9370 | 62.8000 | 62.1830 |

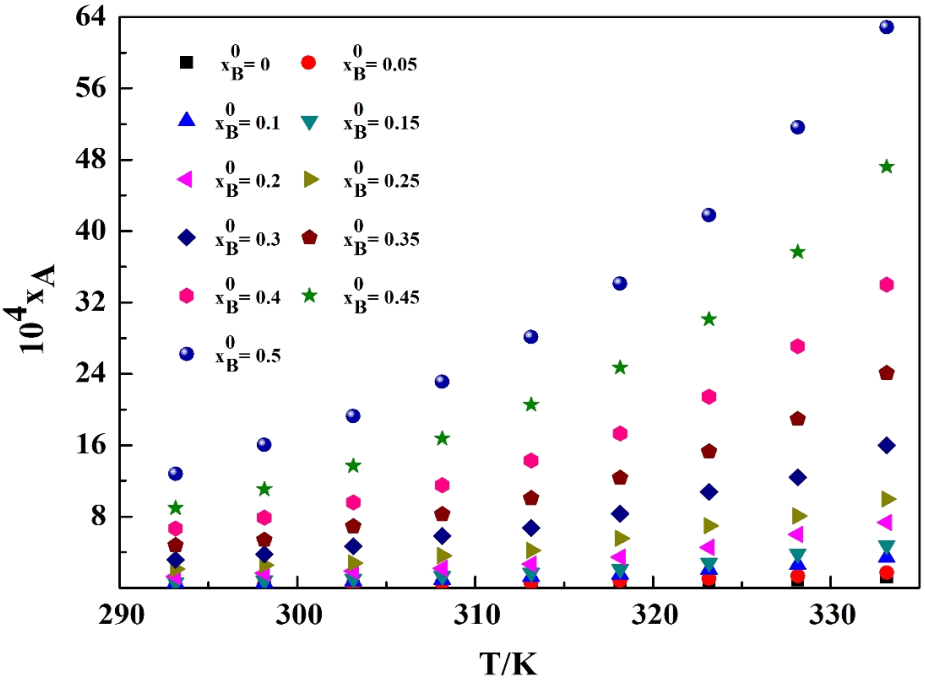


**Figure 2.** Solubility of PRS at different temperatures.

and his colleagues put forward CNIBS/Redlich-Kister formula, which can be written as:

$$lnx_A = x_B^0 ln(x_A)_B + x_C^0 ln(x_A)_C + x_B^0 x_C^0 \sum_{i=0}^{N} S_i (x_B^0 - x_C^0)^i \quad (2)$$

Where $x_A$ represents the mole fraction solubility of PRS, $x_B^0$ and $x_C^0$ are the initial mole fraction of the binary solvents without any solute, $(x_A)_B$ and $(x_A)_C$ are the solubility of solute in pure solvent B and C. In a binary solvent system, N=2 and Equation 2 can be simplified as:

$$lnx_A = B_0 + B_1 x_B^0 + B_2 (x_B^0)^2 + B_3 (x_B^0)^3 + B_4 (x_B^0)^4 \quad (3)$$

Where $B_0$, $B_1$, $B_2$, $B_3$, $B_4$ are the parameters of this model (Acree, 1992; Zhou et al., 2012).

### *3D Jouyban-Acree model*

Jouyban-Acree model was proposed by Jouyban-Gharamaleki and his co-workers (Delgado et al., 2013; Zhao et al., 2016) to discuss the influence of temperature and composition on the solubility of solute in binary solvents, which can be expressed as:

$$lnx_A = x_B^0 ln(x_A)_B + x_C^0 ln(x_A)_C + x_B^0 x_C^0 \sum_{i=0}^{2} \frac{J_i (x_B^0 - x_C^0)^i}{T} \quad (4)$$

When combine Van't Hoff equation with Jouyban-Acree model, $(x_A)_B$ and $(x_A)_C$ can be calculated by the formula:

$$ln(x_A)_B = A_1 + \frac{B_1}{T} \quad (5)$$

$$ln(x_A)_B = A_2 + \frac{B_2}{T} \quad (6)$$

Take Equations 7 and 8 into Equation 6, the 3D Jouyban–Acree model will be obtained as:

$$lnx_A = x_B^0 \left(A_1 + \frac{B_1}{T}\right) + (1 - x_B^0)\left(A_2 + \frac{B_2}{T}\right) + \frac{x_B^0 (1 - x_B^0)}{T} [J_0 + J_1 (2x_B^0 - 1) + J_2 (2x_B^0 - 1)^2] \quad (7)$$

Where $A_1$, $B_1$, $A_2$, $B_2$, $J_0$, $J_1$, $J_2$ represent the model parameters regressed by the experimental data, other characters are the same meaning as Equation 3 (Li et al., 2016; Wang et al., 2014).

### Data correlation

Experimental solubility data and the calculated data were shown in Table 1. Parameters were counted with the 1stOpt software in Table 2-4. Moreover, to verify the applicability and accuracy of these models, root-mean-

**Table 2.** Parameters of the modified Apelblat model for PRS in individual liquid and binary mixtures from 293.15 to 333.15 K at atmospheric pressure.

| $x_B^0$ | A[a] | B[a] | C[a] | $R^{2b}$ | $10^4\sigma_x$[c] | $10^4$RMSD[d] | MD[e] |
|---|---|---|---|---|---|---|---|
| 0 | 456.4032 | -27257.6924 | -66.0459 | 0.9906 | 0.0377 | 0.0355 | 12.0385 |
| 0.05 | -241.0734 | 6577.9277 | 36.6113 | 0.9978 | 0.0240 | 0.0225 | 3.0043 |
| 0.10 | -387.2407 | 13474.5479 | 58.3293 | 0.9980 | 0.0445 | 0.0419 | 3.5088 |
| 0.15 | -331.0875 | 10729.086 | 50.1406 | 0.9984 | 0.0575 | 0.0542 | 2.0581 |
| 0.20 | -498.8888 | 19066.5665 | 74.7956 | 0.9964 | 0.1254 | 0.1183 | 3.2618 |
| 0.25 | -139.3673 | 2730.6000 | 21.3923 | 0.9961 | 0.1714 | 0.1615 | 3.6371 |
| 0.30 | -339.8621 | 12113.7314 | 51.1409 | 0.9971 | 0.2345 | 0.2210 | 2.1371 |
| 0.35 | -380.7834 | 13941.4279 | 57.3123 | 0.9996 | 0.1236 | 0.1164 | 1.1153 |
| 0.40 | -428.6747 | 16188.9655 | 64.4562 | 0.9998 | 0.1144 | 0.1078 | 0.6883 |
| 0.45 | -305.7787 | 10508.2272 | 46.2897 | 0.9995 | 0.2875 | 0.2711 | 1.4235 |
| 0.50 | -220.7555 | 6679.4922 | 33.6808 | 0.9998 | 0.2113 | 0.1992 | 0.7457 |

[a]***A, B, C*:**are the parameters of the modified Apelblat equation;[b]**:** Squared correlation coefficients; [c]$\sigma_x$**:** is the root-mean-square deviation; [d]**RMSD:** is the standard deviation; [e]**MD:** is the mean deviation.

**Table 3.** Parameters of the CNIBS/Redlich-Kister model for PRS in individual liquid and binary mixtures various from 293.15 to 333.15 K at atmospheric pressure.

| T[a]/K | $B_0$[b] | $B_1$[b] | $B_2$[b] | $B_3$[b] | $B_4$[b] | $R^{2\,c}$ | $10^4\sigma_x$[d] | $10^4$RMSD[e] | MD[f] |
|---|---|---|---|---|---|---|---|---|---|
| 293.15 | -11.1593 | 7.9022 | 34.3511 | -119.3479 | 109.9994 | 0.9997 | 0.0777 | 0.0738 | 18.0136 |
| 298.15 | -11.3423 | 17.0753 | -23.6733 | 16.1179 | 4.3545 | 0.9999 | 0.0603 | 0.0575 | 5.4193 |
| 303.15 | -10.6452 | 8.6735 | 18.4859 | -66.3830 | 59.7162 | 0.9998 | 0.0959 | 0.0914 | 5.7201 |
| 308.15 | -10.5797 | 12.2067 | -3.7446 | -14.0511 | 17.6163 | 0.9996 | 0.1446 | 0.1380 | 5.3908 |
| 313.15 | -10.0557 | 8.6700 | 6.8217 | -22.0036 | 14.2802 | 0.9999 | 0.1121 | 0.1070 | 3.5948 |
| 318.15 | -9.8476 | 9.2127 | 5.7887 | -26.5090 | 22.8453 | 0.9999 | 0.1049 | 0.1000 | 2.9231 |
| 323.15 | -9.5421 | 8.8826 | 7.6480 | -34.0207 | 31.4280 | 0.9999 | 0.1343 | 0.1280 | 3.1001 |
| 328.15 | -9.2512 | 9.6070 | -5.3868 | 10.6346 | -12.8317 | 0.9998 | 0.2584 | 0.2464 | 4.8095 |
| 333.15 | -8.9374 | 8.2422 | 0.9490 | 0.5828 | -9.0273 | 0.9997 | 0.3283 | 0.3130 | 4.8787 |

[a]**:** Absolute temperature; [b]**:** Parameters of CNIBS/Redlich-Kister model; [c]**:** Squared correlation coefficients; [d]$\sigma_x$**:** is the root-mean-square deviation; [e]**RMSD:** is the standard deviation; [f]**MD:** is the mean deviation.

**Table 4.** Parameters of the 3D Jouyban-Acree model for PRS in individual liquid and binary mixtures various from 293.15 to 333.15 K at atmospheric pressure.

| $A_1$[a] | $A_2$[a] | $B_1$[a] | $B_2$[a] | $J_0$[a] | $J_1$[a] | $J_2$[a] | $R_2$[b] | $10^4\sigma_x$[c] | $10^4$RMSD[d] | MD[e] |
|---|---|---|---|---|---|---|---|---|---|---|
| 8.0043 | 6.210 | -2995.34 | -5045.3801 | -159.5997 | -1368.3429 | -1388.5474 | 0.9987 | 0.4546 | 0.4521 | 6.5331 |

[a]***$A_1, A_2, B_1, B_2, J_0, J_1, J_2$*:** are the parameters of the 3D Jouyban-Acree model;[b]**:** Squared correlation coefficients; [c]$\sigma_x$**:** is the root-mean-square deviation; [d]**RMSD:** is the standard deviation; [e]**MD:** is the mean deviation.

square deviation $\sigma_x$, standard deviation RMSD, and mean deviation MD were used.

As can be observed, the experimental solubility data were in good agreement with the calculated results, suggesting that these three models were suitable for solubility prediction at different temperature. The maximum $\sigma_x$ values of the Equations 1, 3 and 7 above were $2.875\times10^{-5}$ (modified Apelblat model), $3.283\times10^{-5}$ (CNIBS/Redlich-Kister model) and $4.546\times10^{-5}$ (3D Jouyban-Acree model). Similarly, the maximum RMSD values were $2.711\times10^{-5}$ (modified Apelblat model), $3.130\times10^{-5}$ (CNIBS/Redlich-Kister model) and $4.521\times10^{-5}$ (3D Jouyban-Acree model). Therefore, the modified Apelblat model was more suitable than the other models

**Table 5.** Thermodynamic parameters of PRS in *i*-PrOH and *i*-PrOH/DMF binary solvents at 298.15 K.

| X0 B[a] | $\Delta H_{sol}$[b](kJ mol$^{-1}$) | $\Delta S_{sol}$[c](J mol$^{-1}$K$^{-1}$) | $\Delta G_{sol}$[d](kJ mol$^{-1}$) | $\%\zeta_H$[e] | $\%\zeta_{TS}$[f] |
|---|---|---|---|---|---|
| 0 | 62.90 | 116.85 | 28.07 | 64.36 | 35.64 |
| 0.05 | 36.06 | 34.37 | 25.82 | 77.87 | 22.13 |
| 0.1 | 32.56 | 28.48 | 24.07 | 79.32 | 20.68 |
| 0.15 | 35.09 | 39.36 | 23.35 | 74.94 | 25.06 |
| 0.2 | 26.89 | 17.14 | 21.77 | 84.03 | 15.97 |
| 0.25 | 30.33 | 32.51 | 20.63 | 75.78 | 24.22 |
| 0.3 | 26.06 | 22.11 | 19.46 | 79.81 | 20.19 |
| 0.35 | 26.16 | 25.53 | 18.54 | 77.46 | 22.54 |
| 0.4 | 25.18 | 25.17 | 17.68 | 77.04 | 22.96 |
| 0.45 | 27.38 | 35.34 | 16.84 | 72.21 | 27.79 |
| 0.5 | 27.96 | 40.11 | 16.00 | 70.04 | 29.96 |

[a]: The mole fraction of DMF in the binary solvents without any solute; [b]: Standard enthalpy of solution of PRS; [c]: Standard entropy of solution of PRS; [d]: Molar Gibbs free energy change of solution of PRS; [e]: Relative contributions of the enthalpy; [f]: Relative contributions of the entropy.

for correlating the solubility data of PRS.

**Thermodynamic properties of solutions**

The data showed above indicated that the solubility of PRS was influenced by both the temperature and the composition of the solvent system. Consequently, the standard enthalpy, entropy and molar Gibbs free energy change of solution of PRS in various solvent systems can be calculated by Equations 8-10, which were derived from the modified Van't Hoff equation and the Apelblat model (Perlovich et al., 2004; Sun et al., 2016; Yang et al., 2016).

$$\Delta H_{sol} = RT(C - B/T) \quad (8)$$

$$\Delta S_{sol} = R(A + C + ClnT) \quad (9)$$

$$\Delta G_{sol} = -RT(A + B/T + ClnT) \quad (10)$$

Where $\Delta H_{sol}$, $\Delta S_{sol}$ and $\Delta G_{sol}$ represent the standard enthalpy, entropy and molar Gibbs free energy change of solution of PRS, respectively. *A*, *B*, and *C* are the parameters of the modified Apelblat model. T is 298.15K, which is the standard temperature within the experimental temperature range of 293.15-333.15K.

The relative contributions of the enthalpy and entropy to the standard free energy of solution can be calculated by Equations 11 and 12.

$$\%\zeta_H = 100 \times \frac{|\Delta H_{sol}|}{|\Delta H_{sol} + T\Delta S_{sol}|} \quad (11)$$

$$\%\zeta_{TS} = 100 \times \frac{|T\Delta S_{sol}|}{|\Delta H_{sol} + T\Delta S_{sol}|} \quad (12)$$

Where $\%\zeta_H$ and $\%\zeta_{TS}$ are the relative contributions of the enthalpy and entropy respectively. Values of $\Delta H_{sol}$, $\Delta S_{sol}$,$\Delta G_{sol}$, $\%\zeta_H$ and $\%\zeta_{TS}$ were calculated and shown in Table 5.

As seen in Table 5, the standard enthalpy was positive, indicating that the dissolution of PRS in *i*-PrOH and *i*-PrOH/DMF binary solvents were an endothermic process, which explained why the mole fraction solubility increased along with the temperature. When the fraction of DMF ($x_B^0$) increased in the binary mixtures, the solubility of the solute increased with the decreasing enthalpy, suggesting that the dissolution process was enthalpy-controlled. The maximum standard enthalpy was found at the lowest mole fraction of DMF, so was the entropy. It should be mentioned that the changes in enthalpy and entropy of dissolution had a local maximum at a content of 0.1-0.15 mole fractions of DMF. The value of the enthalpy for the solution process is the integration of several kinds of interactions, thus the higher values of the enthalpy indicated that more energy was needed to overcome the cohesive force of the solute and the solvent in this region. Meanwhile, Equations 8-10 derived from the modified Van't Hoff equation and the Apelblat model has the limit of considering only temperature effect, resulting in the inaccuracy for systems which were also solvent composition dependent.

The dissolution process was non-spontaneous because the molar Gibbs free energy change of solution was positive. Besides, the relative contributions of the enthalpy and entropy to the standard free energy of solution suggested that main contributor was the enthalpy during the dissolution of PRS in the mixture solvents

studied.

## Conclusion

The solubility of PRS in *i*-PrOH and *i*-PrOH/DMF mixture solvents (293.15 to 333.15K) was measured at atmospheric pressure using the dynamic laser method. The mole fraction solubility of PRS in the mixture solvents increased with the temperature and the mole fraction of DMF. Experimental data were correlated by the modified Apelblat equation, the CNIBS/Redlich-Kister model and 3D Jouyban-Acree model. It turned out that all the models were well fitted. Moreover, thermodynamic properties, such as the standard enthalpy, entropy and molar Gibbs free energy change of solution were calculated by the modified Van't Hoff equation and the Apelblat model. In conclusion, the dissolution process was an endothermic and non-spontaneous process, and depended on enthalpy.

## ACKNOWLEDGEMENTS

This work was supported by National Natural Science Foundation of China (No. 21576080) and the Fundamental Research Funds for the Central Universities (No. 222201714036).

## List of symbols

| | |
|---|---|
| $x_A$ | Mole fraction of solute |
| $m_a$, $m_b$, $m_c$ | Masses of solute and solvents B and C, respectively, g |
| $M_A$, $M_B$, $M_C$ | Molecular weights of solute and solvents B and C, respectively, g mol$^{-1}$ |
| $T$ | absolute temperature, K |
| $\boldsymbol{x_B^0}$ | *N,N*-dimethylformamide mole fraction in binary solvents without solute |
| $R^2$ | Squared correlation coefficients |
| $\sigma_x$ | Root-mean-square deviation |
| RMSD | standard deviation |
| *MD* | Mean deviation |
| $x_A$, *xcal A* | Experimental and calculated values |
| $\Delta H_{sol}$ | Enthalpy of dissolution, kJ mol$^{-1}$ |
| $\Delta S_{sol}$ | Entropy of dissolution, J mol$^{-1}$ |
| $\Delta G_{sol}$ | Gibbs free energy of dissolution, kJ mol$^{-1}$ |
| $R$ | Gas constant (8.314 J mol$^{-1}$ K$^{-1}$) |
| $\%\zeta_H$ | Partial enthalpy contribution |
| $\%\zeta_{TS}$ | Partial entropy contribution |

## REFERENCES

Delgado D. R., Rodriguez G. A., Holguin A. R., Martinez F. and Jouyban A. (2013). Solubility of sulfapyridine in propylene glycol plus water mixtures and correlation with the Jouyban-Acree model. Fluid Phase Equilibr. 341:86-95.

Furuta H., Mori S., Yoshihashi Y., Yonemochi E., Uekusa H., Sugano K.& Terada K. (2015a). Physicochemical and crystal structure analysis of pranlukast pseudo-polymorphs I: anhydrates and hydrate. J. Pharm. Biomed. Anal. 107:11-16.

Furuta H., Mori S., Yoshihashi, Y., Yonemochi, E., Uekusa, H., Sugano, K. & Terada K. (2015b). Physicochemical and crystal structure analysis of pranlukast pseudo-polymorphs II: Solvate and cocrystal. J. Pharm. Biomed. Anal. 111:44-50.

Ge L., Bao A. & Yang K. (2016). Determination and correlation of the solubility for Berberine chloride in pure imidazolium-based ionic liquids. J. Chem. Eng. Data. 61(5):1829-1835.

Hong M., Wu S., Qi, M. & Ren, G. (2016). Solubility correlation and thermodynamic analysis of two forms of Metaxalone in different pure solvents. Fluid Phase Equilibr. 409:1-6.

Jouyban-Gharamaleki V., Jouyban-Gharamaleki K., Soleymani J., Acree W. E. & Jouyban A. (2014). Solubility determination of Tris(hydroxymethyl)aminomethane in water + methanol mixtures at various temperatures using a laser monitoring technique. J. Chem. Eng. Data. 59(7):2305-2309.

Li S., Jiang L., Qiu J.& Wang P. (2016). Solubility and solution thermodynamics of the δ form ofl-citrulline in water + ethanol binary solvent mixtures. J. Chem. Eng. Data. 61(1):264-271.

Li T., Jiang Z.-x., Chen F.-x. & Ren B.-z. (2012). Solubilities of d-xylose in water+(acetic acid or propionic acid) mixtures at atmospheric pressure and different temperatures. Fluid Phase Equilibr. 333:13-17.

Perlovich G. L., Kurkov S. V., Kinchin A. N. & Bauer-Brandl A. (2004). Thermodynamics of solutions III: comparison of the solvation of (+)-naproxen with other NSAIDs. Eur. J. Pharm. Biopharm. 57(2):411-420.

Qiaoli Chen Y. W., Yanbin L. & Jingkang W. (2009). Solubility and metastable zone of cefoperazone sodium in acetone water system. J. Chem. Eng. Data. 54:1123-1125.

Sun H., Liu B., Ren K. & Li J. (2016). Solubility of d-phenylglycine methyl ester hydrochloride in water and in organic individual or mixed solvents: Experimental data and results of thermodynamic modeling. Fluid Phase Equilibr. 417:62-69.

Wang P., Jiang J., He L., Li H., Li J., Liu J.& Zhao Y. (2013). Solubility of Isomalt in the Water + Ethanol Solvent System at (288.15, 298.15, 308.15, and 318.15) K. J. Chem. Eng. Data. 58(2):364-369.

Wang P., Jiang J., Jia X. A., Jiang L.& Li S. (2014). Solubility of trehalose in water + ethanol solvent system from (288.15 to 318.15) K. J. Chem. Eng. Data. 59(6):1872-1876.

Acree W. E. Jr. (1992). Mathematical representation of thermodynamic properties Part 2. Derivation of the combined nearly ideal binary solvent (NIBS)/Redlich-Kister mathematical representation from a two-body and three-body interactional mixing model. Thermochimica Acta. 198:71-79.

Yang X., Wang J., Song H. & Zou W. (2016). Thermal properties and solubility of methyl α-d-glucopyranoside in methanol at different temperatures. Fluid Phase Equilibr. 409:417-424.

Yoshihara S. (2013). Pranlukast hydrate in the treatment of pediatric bronchial asthma. Pediatr. Health. Med Ther. 4:55-63.

Yu Z. Q., Chew J. W., Chow P. S. & Tan R. B. H. (2007). Recent advances in crystallization control. Chem. Eng. Res. Des. 85(7):893-905.

Zhao K., Lin L., Li C., Du S., Huang C., Qin Y. & Gong J. (2016). Measurement and correlation of solubility of γ-aminobutyric acid in different binary solvents. J. Chem. Eng. Data. 61(3):1210-1220.

Zhou X., Fan J., Li N., Du Z., Ying H., Wu J. & Bai J. (2012). Solubility of l-phenylalanine in water and different binary mixtures from 288.15 to 318.15K. Fluid Phase Equilibr. 316:26-33.

Zhu P., Chen Y., Zhou Y., Xiao Y., Ouyang J., Huang X. & Chen W. (2016). Thermodynamics of 1,3-Dimethylurea in eight alcohols. J. Chem. Eng. Data. 61(4):1517-1523.

Zhi J., Liu Q., Li T. & Ren B. (2016). Measurement and correlation of the solubility for camptothecine in different organic solvents. J. Chem. Eng. Data. 61(6):2052-2061.